Spectroscopy of electronic states in InAs quantum dots grown on In(x)Al(1-x)As/InP(001)

F. Fossard, A. Helman, G. Fishman, F. H Julien, J. Brault, M. Gendry, Emmanuel Peronne, Antigoni Alexandrou, S. E Schacham, G. Bahir, et al.

Spectroscopy of the electronic states in InAs quantum dots grown on $In_xAl_{1-x}As/InP(001)$

F. Fossard,* A. Helman, G. Fishman, and F. H. Julien
Institut d'Electronique Fondamentale, UMR 8622 CNRS, Université Paris XI, 91405 Orsay Cedex, France

J. Brault and M. Gendry
Laboratoire d'Electronique-LEOM, UMR 5512 CNRS, Ecole Centrale de Lyon, 69134 Ecully Cedex, France

E. Péronne and A. Alexandrou
Laboratoire d'Optique et Bioscience, UMR 7645 CNRS, Ecole Polytechnique-Ensta, 91128 Palaiseau Cedex, France

S. E. Schacham
Department of Electrical and Electronical Engineering, College of Judea and Samaria, Ariel 44837, Israel

G. Bahir and E. Finkman
Department of Electrical Engineering and Solid State Institute, Technion, Haifa 32000, Israel
(Received 13 May 2003; published 29 April 2004)

We have investigated optical properties of high-density InAs self-assembled quantum dots (QDs) in an $In_xAl_{1-x}As$ matrix, lattice matched to an InP (001) substrate. The weak lattice mismatch ($\sim 3\%$) results in a 90% coverage of the $In_xAl_{1-x}As$ surface with InAs QDs. By means of interband and intraband spectroscopies crossed with atomic force microscopy (AFM) measurements, we have determined that the InAs QDs optical properties depend on the deposited amount of InAs. Photoinduced absorption spectroscopy has been used to investigate midinfrared intraband absorptions. For three monolayers (ML) InAs deposit thickness, just above two-dimensional (2D)/3D growth mode transition (2.5 ML), the islands form as isolated elliptical dots elongated along the $[1\bar{1}0]$ direction and exhibit intraband resonances polarized either along the [110] or the $[1\bar{1}0]$ direction. For thicker deposition (>3 ML), InAs islands form chains of elliptical dots along the $[1\bar{1}0]$ direction where the quantum confinement is lost, resulting in a quantum-wire-like behavior. In this paper, we also report on photoluminescence and photocurrent spectroscopies, in order to get insight into the $InAs/In_xAl_{1-x}As$ island band structure. These experimental results are in good agreement with that of a multiband $\mathbf{k}\cdot\mathbf{p}$ model.

DOI: 10.1103/PhysRevB.69.155333 PACS number(s): 78.67.Hc, 78.55.Cr, 73.21.La, 07.57.Ty

I. INTRODUCTION

Quantum dots (QDs) are of key interest for applications to infrared (IR) optoelectronics such as IR photodetectors,[1] IR lasers,[2] or basic single-photon emission devices.[3] The electronic and optical properties of zero-dimensional (0D) semiconductors are fundamentally different from those of 1D, 2D, and bulk semiconductors. The three-dimensional confinement of the carriers results in an atomlike density of states $\delta(E)$. The discretization of the density of states was predicted to slow down the interlevel relaxation of the carriers.[4] This so-called ''phonon bottleneck'' effect,[5] which has been recently revisited in terms of polaron relaxation due to the strong electron-phonon coupling in QDs,[6–8] can improve the quantum efficiency of unipolar devices such as quantum dot infrared photodetectors[9] (QDIP) or quantum cascade lasers.[10] Moreover, the in-plane confinement of the carriers allows the intraband absorption or the emission of photons at normal incidence, which is forbidden in quantum wells. In order to obtain a better efficiency, a high density of dots is required as well as a large oscillator strength of the intraband optical transition. In previous works, we showed that the self-organized growth in the $InAs/In_{0.52}Al_{0.48}As/InP(001)$ system results in a high density of InAs quantum islands[11] and that strong intraband resonances take place at wavelengths of 14–15 μm with a polarization in the layer plane along the [110] axis.[12]

In this paper, we report on intraband spectroscopy of self-organized InAs QDs grown on $In_{0.52}Al_{0.48}As/InP(001)$. We show that the quantum islands morphologies and their associated physical properties can be varied, according to the amount of InAs deposited. When the thickness of InAs is equal to three monolayers (ML), we obtain isolated QDs elongated in the $[1\bar{1}0]$ direction. When the InAs thickness is increased by only 0.5 ML, QDs connect and form linear chains along the same $[1\bar{1}0]$ direction. The quantum structures have a different optical behavior related to their isolated or connected nature. In isolated dots, we present evidence of the quantum confinement of the carriers in the [110] and $[1\bar{1}0]$ directions. We then show that the confinement along the $[1\bar{1}0]$ direction is lost in the chains of dots and that intraband resonances are narrower than in isolated dots. This indicates a smaller size dispersion of the chains of dots. In order to reconstruct the energy diagram of the dots, photocurrent spectroscopy of the dots has been performed to assess the ground-state energy. We also present a two-band $\mathbf{k}\cdot\mathbf{p}$ model which is in agreement with the experimental data.

TABLE I. Growth parameters for the four samples studied in this work.

Sample	n doping (cm^{-2})	InAs thickness (nm)
A	No	0.9
B	5×10^{11}	0.9
C	No	1.05
D	1×10^{12}	1.05

II. SAMPLE GROWTH

The four samples, labeled *A* to *D*, studied in this work (see Table I) were grown at 525 °C on semi-insulating InP substrates using solid-source molecular-beam epitaxy. All samples consist in an $In_{0.52}Al_{0.48}As$ ($In_xAl_{1-x}As$) buffer layer lattice matched to InP, an active region containing 10 planes of InAs QDs separated by 50-nm-thick $In_xAl_{1-x}As$ spacer layers, and a 300-nm $In_xAl_{1-x}As$ cap layer. For InAs/$In_xAl_{1-x}As$ QDs, it is possible, by the control of the InAs surface reconstruction [(2×4) or (2×1)] and the $In_xAl_{1-x}As$ surface preparation (growth interruption time, under arsenic flux, before the InAs growth), to obtain either wires or elongated dots.[11,12] In this work, the InAs growth conditions [growth temperature and arsenic pressure favoring (2×1) reconstruction] and the $In_xAl_{1-x}As$ surface preparation (growth interruption time of 600 s) were chosen to favor the formation of InAs elongated dots. Our attention is especially focused on the deposited amount of InAs. For samples *A* and *B* (*C* and *D*), the thickness of InAs deposited in each plane is 0.9 nm (1.05 nm) corresponding to 3 (3.5) ML. Sample *B* contains lattice-matched $In_{0.53}Ga_{0.47}As$ contact layers which were grown at the bottom (500 nm *n*-doped at 8×10^{18} cm^{-3}) and the top (500-nm *n*-doped at 10^{18} cm^{-3}) of the structure for photocurrent spectroscopy purposes. For this sample, the $In_xAl_{1-x}As$ spacer layers were δ-doped at the center with silicon to achieve a sheet carrier density of 5×10^{11} cm^{-2}. For sample *D*, δ doping is performed 15 nm below and above the InAs layer to achieve a sheet carrier density of 1×10^{12} cm^{-2}.

III. ISOLATED ELONGATED DOTS

Figure 1 shows the photoluminescence (PL) spectrum of sample *A* at 77 K. The optical excitation is provided by an argon laser. The low excitation spectrum ≈40 W cm^{-2} (dotted curve) reveals a structured peak at 1.1 eV with a full width at half maximum (FWHM) of 124 meV, reflecting the size dispersion of the dots. Weber *et al.* showed that the structure of the PL is mainly related to various dot heights corresponding to an integer number of ML and also to excited states.[13]

Under intense excitation ≈1.5 kW cm^{-2}, the PL spectrum (solid curve) reveals that the high-energy side of the peak increases with the excitation intensity. The PL FWHM is 139 meV, which is 11% larger than that under low excitation conditions. The optical excitation provides electron-hole pairs in the dots and in the barriers. The filling of the dots is a result of complex processes which involve transport and capture of the carriers. However, at high excitation, the ground state of the dots is full and the increase of the high-energy side of the peak can be attributed to optical recombination between excited states of the dots.[14–16] This last result demonstrates the dotlike behavior of this type of InAs islands. The global broadening of the PL spectrum, at high energy, is an indication of the filling of either the excited states of the large dots or the ground state of the small dots.

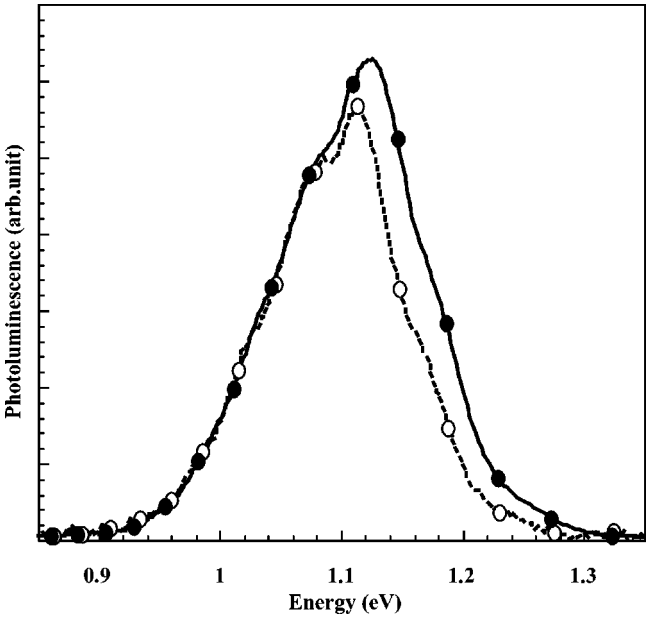

FIG. 1. 77 K photoluminescence spectra of sample *A* at low excitation (dotted curve) and high excitation (solid curve).

Since intraband transitions are polarized along the confinement direction, we expect to observe intraband absorptions for both in-plane polarizations ([110] and $[1\bar{1}0]$). Thus, it is difficult to perform standard transmission measurements due to the lack of ideal reference. Intraband experiments were first performed using photoinduced absorption (PIA) spectroscopy. The sample is optically excited by a chopped argon laser to generate electron-hole pairs. The resulting intraband absorption is probed using a Fourier transform infrared spectrometer operating in step-scan mode and using standard lock-in techniques.[17] The density of carriers generated by the excitation (10^9-10^{10} cm^{-2}) is negligible compared to the intentional doping. As the reference spectrum is provided by a transmission of the same sample without optical excitation, this method does not require a separated undoped sample as a reference. This very sensitive method allows the observation of absorption as weak as 10^{-6}.

Figure 2(a) shows the PIA spectra of sample *B* at normal incidence at 77 K for two in-plane polarizations. The top $In_xGa_{1-x}As$ layer of the sample was chemically etched to reduce free-carrier absorption and to allow optical excitation of the active layer. The [110] polarized spectrum shows a narrow absorption at 87 meV with a FWHM of 13 meV. A second peak, ten times smaller, occurs at 120 meV with a FWHM of about 30 meV. The $[1\bar{1}0]$ polarized spectrum exhibits two absorptions. On the low-energy side, one can

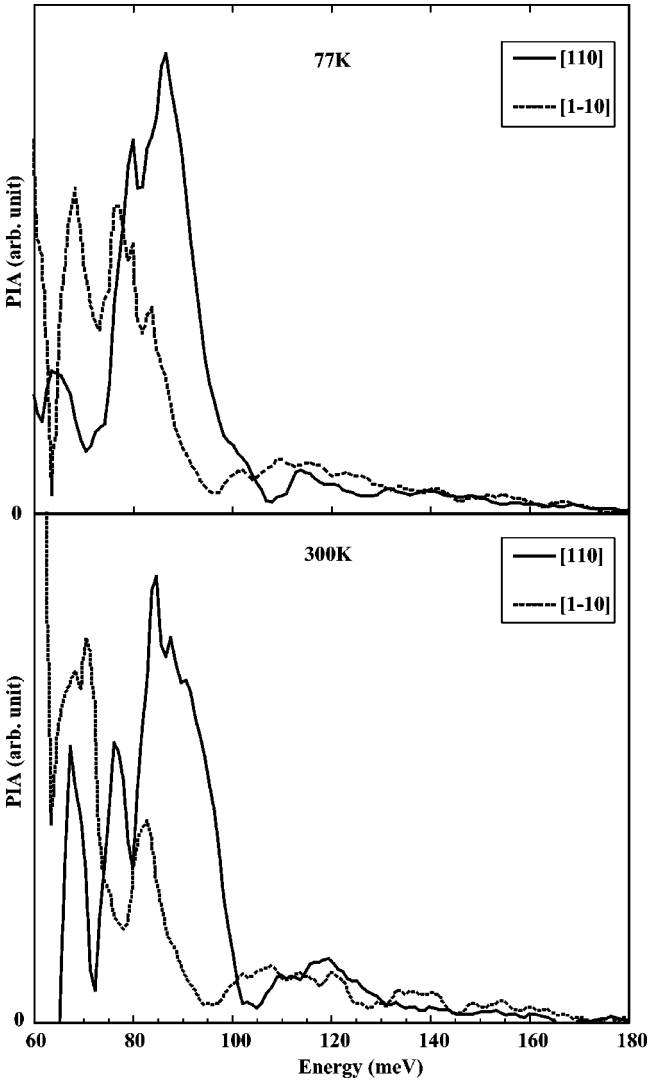

FIG. 2. Photoinduced absorption spectra of sample *B* at normal incidence for two orthogonal in-plane polarizations. Absorptions were probed at 77 K (upper graph) and 300 K (bottom graph).

see the onset of an absorption at 80 meV with a FWHM of the order of 20 meV. The sharp notches near 78, 82, and 86 meV are due to two-phonon absorptions in the InP substrate. The 80-meV peak is not related to free-carrier absorption because it is only observed for one polarization. Note that a second peak, at higher energy, occurs at 108 meV with a FWHM of about 30 meV. Figure 2(b) shows the PIA spectra at normal incidence of sample *B* at 300 K. With increasing temperature, each transition is redshifted by 2–3 meV, which is typical of interlevel transitions.[18] For both polarizations, the relative intensity of the high-energy absorptions compared to the low-energy absorptions increases by 40%. This result has been confirmed by normal incidence transmission measurements at 77 and 300 K. This reveals that the high-energy transitions occur between excited states of the dots. With the temperature increase, the first excited states (*p* states) are filled with more carriers. Thus, the absorption from the ground state is reduced while the absorption from excited *p* states is increased. As the dots have a preferential

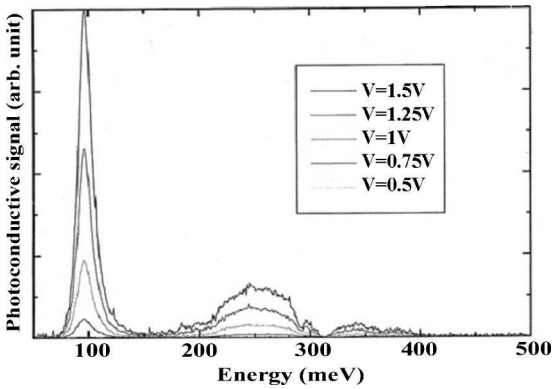

FIG. 3. Normal incidence photocurrent spectra of sample *B* at 15 K as a function of the incident light energy for several biases applied to the structure.

orientation, we can attribute the observed low-energy resonances in $[110]$ ($[1\bar{1}0]$) to transitions from the ground state *s* to an excited state *p* with an envelope wave function with one node along the $[110]$ ($[1\bar{1}0]$) axis. High-energy absorptions can be related to transitions from a *p* state with one node along the $[110]$ ($[1\bar{1}0]$) axis to a higher excited stated with two nodes along the $[110]$ ($[1\bar{1}0]$) axis.

Additional photocurrent (PC) experiments[19] were performed at normal incidence (front illumination) on sample *B*. PC measurements are important for QDIPs applications and also provide more insight since we observe more transitions than in absorption measurements. Figure 3 shows the photocurrent spectrum as a function of the energy of the incident radiation for different bias applied to the structure. The spectra exhibit two main structures which behave differently. On the high-energy side, we can notice a broad peak at 250 meV. The peak of the photoconductive current depends linearly on the applied bias which is typical of bound to continuum transitions. Thus, it reveals that the ground state of the dots in sample *B* lays 250 meV below the continnum.[20] On the low-energy side, a structure appears at 95–100 meV and has a superlinear dependence with the bias. Such behavior is expected for a bound to bound transition since the tunneling probability of the carriers from the upper bound level into the continuum increases as the barrier becomes more slanted. We can easily link this peak to the intense absorptions observed at the same energy in PIA experiments. Since this transition is followed by tunneling, its amplitude is thus reduced, and becomes comparable to that of the higher energy in spite of its very large oscillator strength.

IV. CHAINS OF ELONGATED DOTS

Figure 4 shows the photoluminescence spectra of sample *C* at 77 K for two excitation intensities. At low excitation (dotted curve), the luminescence is peaked at 1.03 eV with a FWHM of 117 meV. It should be noticed that the PL occurs at a lower energy with respect to isolated dots. This energy reduction is related to the increased dot height, as expected from the larger amount of the InAs deposited in this sample.

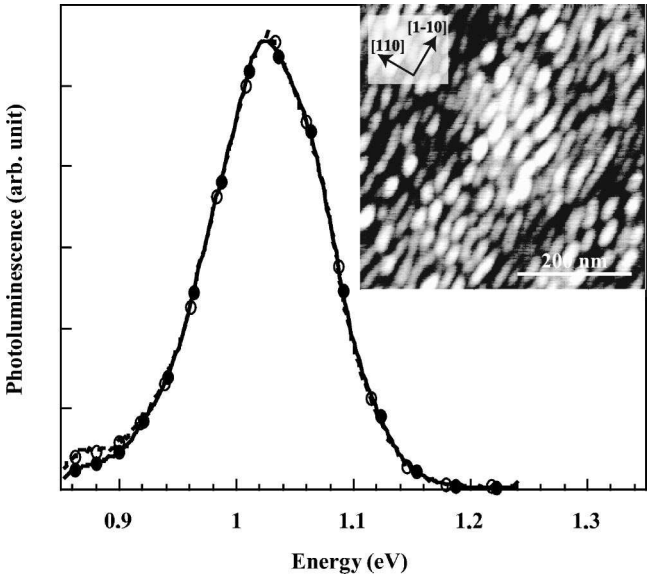

FIG. 4. 77 K photoluminescence spectra of sample *C* at low excitation (dotted curve) and high excitation (solid curve). The inset shows a typical AFM image of an uncapped sample.

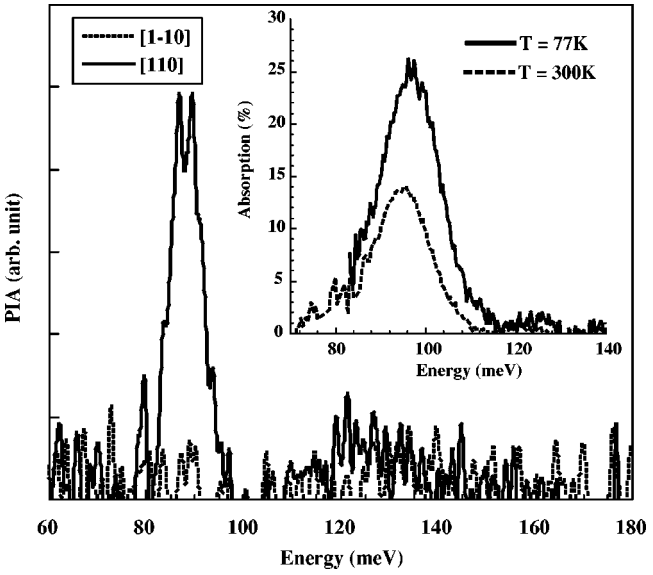

FIG. 5. Normal incidence photoinduced absorption spectra of sample *C*, at 77 K, for polarizations [110] and $[1\bar{1}0]$. The inset shows the absorption of sample *D*, at normal incidence, as a function of the photon energy at 77 and 300 K.

We estimate that, in this sample, the dots are about 1 ML higher than in sample *B*.

The solid curve of Fig. 4 shows the PL spectrum of sample *C* under high excitation. The shape of the PL peak is basically unchanged with increasing excitation density. In contrast to the isolated dots, the chains of dots do not exhibit hot photoluminescence from the excited states. This behavior suggests a quantum-wire-like type of confinement. Indeed, in a quantum wire, even if the density of state is peaked at $k=0$, there is still room for carriers in the ground subband. This point clarifies the ambiguous behavior of the InAs QDs grown on $In_xAl_{1-x}As$ already mentioned by Weber *et al.*[13]

Figure 5 shows the 77 K PIA spectra of sample *C* at normal incidence, respectively, for light polarized along the [110] and $[1\bar{1}0]$ directions of the layer plane. The [110] polarized spectrum reveals an intense and narrow absorption at 90 meV with a small FWHM of 7.5 meV. This resonance can be attributed to the intraband transition between the ground state and the first excited state related to the confinement of the electron along [110]. Within experimental accuracy, no absorption is observed for a polarization along the $[1\bar{1}0]$ direction in the investigated spectral range.

The inset of Fig. 5 shows the absorption spectra at normal incidence of the *n*-doped sample *D* as a function of temperature. At 77 K, the absorption reaches the record value of 26% at 95 meV (12.8 μm) with a 16 meV FWHM. According to Weber *et al.*, it is clear that the observed transition occurs in the conduction band. The absorption of one plane *A* can be approximated by

$$A = 1 - e^{-N_p \sigma \rho_S}$$

with σ the absorption cross section and ρ_S the 2D carrier density. We deduce the oscillator strength f of the transition from[21]

$$f = \frac{nc\varepsilon_0 m_0 \sigma}{e^2 \hbar} \zeta$$

with the refractive index n of InAs, the speed of light c, the electric constant ε_0, the electronic mass m_0, the elementary charge e, and the FWHM of the transition ζ. The obtained value is of the order of 21. Note that this large value is likely to be underestimated because we assumed that all electrons are trapped in the dots. One should also take into account the band bending in heavily doped heterostructures. δ doping in the barrier creates a depletion region and band bending which may reduce the probability of electrons to be localized on a confined level.

The inset of Fig. 5 also shows that the integrated absorption drops by 32% when the temperature is increased from 77 K to room temperature. Populations of the upper and ground states are estimated, as a first approximation, assuming a 1D-subband effective-mass model. The Fermi level ε_F verifies

$$N_{1D} = \int_0^\infty \rho(\varepsilon) \frac{1}{1+\exp\left(\frac{\varepsilon - \varepsilon_F}{k_B T}\right)} d\varepsilon,$$

where $\rho(\varepsilon)$ is the density of state in a wire, N_{1D} is the density of carriers in a wire, and k_B is the Boltzmann constant. We deduce the population of the two levels from this calculus and evaluate the absorption. Results confirm that the absorption is expected to drop by 30% when the temperature is increased from 77 to 300 K. Intraband spectroscopy confirms the wirelike behavior of the chains of elongated dots since no absorption is observed in the $[1\bar{1}0]$ direction. The connec-

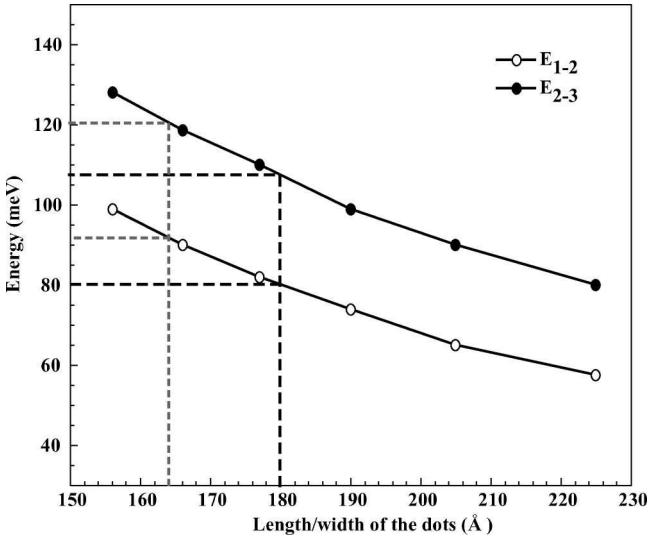

FIG. 6. Calculated energies of the E_{12} and E_{23} intraband transitions as a function of the in-plane dimension of the dot.

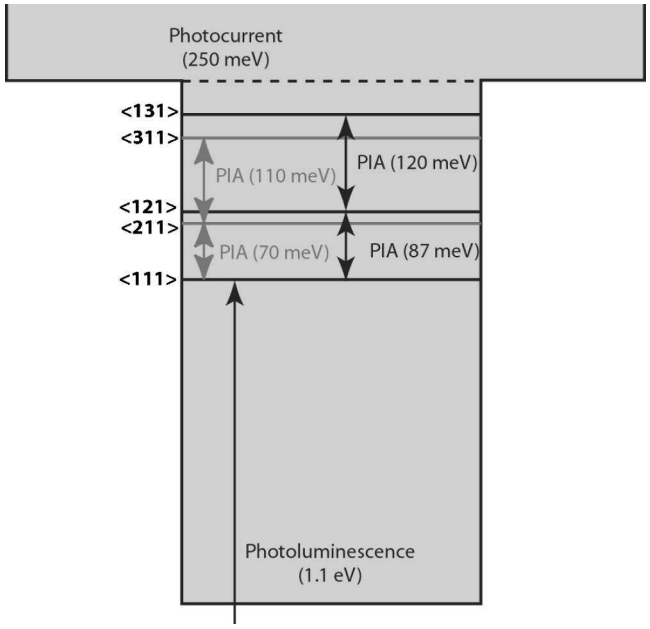

FIG. 7. Energy diagram of the isolated elongated dots. Each level is labeled with three quantum numbers X, Y, and Z indicating the number of nodes along the $[1\bar{1}0]$, [110], and [001] direction, respectively.

tion of the dots along the big axis $[1\bar{1}0]$, as indicated by the atomic force microscopy (AFM) image, induces the formation of short wires.

V. MODEL AND ENERGY DIAGRAM

At the vicinity of $k=0$, the band structure of a semiconductor can be approximated by a parabolic dispersion curve but in the range of a few percent of the Brillouin zone only. The nonparabolicity becomes stronger in narrow-gap semiconductors such as InAs. Therefore, it is inaccurate to use a one-band model to simulate the energy structure of the isolated elongated dot. Since we are mainly interested in the electron states, a good approximation of the conduction band is required. First of all, we calculate the bulk dispersion of the InAs with the eight-band matrix of Pidgeon and Brown[22] using the Luttinger parameters given by Boujdaria *et al.*[23] We then use a two-band $\mathbf{k}\cdot\mathbf{p}$ matrix to fit the correct conduction band within the first 10% of the Brillouin zone.

Since the exact shape of the dots is unknown, as well as their large size dispersion, a few approximations were made to simplify the calculations. Variable separation was used for X, Y, and Z. The shape of the truncated pyramidal dot can be approximated by a rectangular box with the same volume. The energy of the electrons is assumed to be the sum of the confinement in three quantum wells representing the confinement along the three axes of the dots: [110], $[1\bar{1}0]$, and [001].

We chose to describe each band with a base of sine functions, as described in Ref. 24, which simplifies the calculation of the derivatives and integrals in each matrix element. In order to obtain a good description of the energy, the model requires quite a large base with each band described by 30 sine functions. This procedure leads to an accuracy of about 1 meV. For the two-band model described above, the size of the matrix is then 60×60.

Results of the calculation are illustrated in Fig. 6. The curves show the calculated energy transitions E_{1-2} and E_{2-3} depending on the confinement direction of the plane. Note that for a length of 180 Å, E_{1-2} and E_{2-3} are calculated, respectively, as 80 and 108 meV; and for a width of 164 Å, E_{1-2} and E_{2-3} are calculated, respectively, as 91 and 118 meV. Moreover, we calculated the position of the electronic ground state of the dots and we obtained values between 220 and 320 meV. Once again, the calculated value is close to the experimental value. Equivalent values have been calculated using an eight-band model. It demonstrates that the two-band model allows a good description of the electronic states.

The good agreement between the calculation and the experiments allows us to construct the energy diagram of the dots. The resonances observed at low energies in both polarizations are attributed to intraband transitions between the *s* ground state of the dots and the first *p* excited state (envelope wave function with one node in the layer plane) relative to the confinement along the [110] and $[1\bar{1}0]$ directions. Moreover, the high-energy absorption peaks can be attributed to transitions starting from *p* states to *d* states (two nodes in the layer plane).[25] Figure 7 summarizes the energy diagram of the isolated elongated dots. We chose to label the electronic state with three quantum numbers representing the number of nodes in the three directions X, Y, and Z which correspond to crystallographic directions $[1\bar{1}0]$, [110], and [001], respectively.

VI. CONCLUSION

In this paper, we report on optical spectroscopy of InAs quantum islands grown on $In_xAl_{1-x}As$ lattice matched to InP(001). Samples containing different types of InAs islands

have been studied by photoluminescence, infrared spectroscopy, and photocurrent spectroscopy. All samples show strong midinfrared intraband absorptions at normal incidence. We have shown that the optical behavior of the islands is affected by the amount of InAs deposited. When the thickness of InAs (3 ML) is just above the 2D/3D transition (2.5 ML), the islands behave like quantum dots. The observation of giant s-p resonances in the 12–20 μm region and weaker p-d absorptions in the 8–12-μm region has confirmed the three-dimensional confinement of the islands. Added to photocurrent spectroscopy, these results have allowed the reconstruction of the energy diagram of the dotlike InAs islands.

On the other hand, when the amount of InAs deposited reaches 3.5 ML, the discrete signature disappears and the InAs islands behave like quantum wires. This effect is attributed to the connection of the dots along the $[1\bar{1}0]$ axis. Moreover, the optical spectroscopy of these strings reveals a weaker size dispersion related to the FWHM of the spectra. Infrared spectroscopies have shown that the intraband absorption reaches a record value of 26% for 10 planes of n-doped (10^{12} cm^{-2}) chains of elongated dots. The FWHM of the intraband absorption is as small as 7.5 meV at 13.5 μm in undoped samples.

We have shown that the energy structure of the isolated elongated dots can be described by a simple two-band $\mathbf{k}\cdot\mathbf{p}$ model which takes into account the strong nonparabolicity in InAs. Calculations show good agreement with the experimental data.

ACKNOWLEDGMENT

The authors would like to thank J. P. Leburton for fruitful discussions.

*Corresponding author. Electronic address: frederic.fossard@ief.u-psud.fr

[1] B. F. Levine, J. Appl. Phys. **74**, R1 (1993).
[2] Y. Arakawa and H. Sasaki, Appl. Phys. Lett. **40**, 939 (1982).
[3] A. Imamoglu and Y. Yamamoto, Phys. Rev. Lett. **72**, 210 (1994).
[4] U. Bockelmann and G. Bastard, Phys. Rev. B **42**, 8947 (1990).
[5] H. Benisty, C. M. Sotomayor-Torrès, and C. Weisbuch, Phys. Rev. B **44**, 10 945 (1991).
[6] S. Hameau, Y. Guldner, O. Verzelen, R. Ferreira, G. Bastard, J. Zeman, A. Lemaître, and J. M. Gérard, Phys. Rev. Lett. **83**, 4152 (1999).
[7] S. Hameau, J. N. Isaia, Y. Guldner, E. Deleporte, O. Verzelen, R. Ferreira, G. Bastard, J. Zeman, and J. M. Gérard, Phys. Rev. B **65**, 085316 (2002).
[8] O. Verzelen, R. Ferreira, and G. Bastard, Phys. Rev. B **62**, 4809 (2000).
[9] E. Finkman, S. Maimon, V. Immer, G. Bahir, S. E. Schacham, O. Gauthier-Lafaye, S. Herriot, F. H. Julien, M. Gendry, and J. Brault, Physica E (Amsterdam) **7**, 139 (2000).
[10] C. Becker, C. Sirtori, O. Drachenko, V. Rylkov, D. Smirnov, and J. Leotin, Appl. Phys. Lett. **81**, 2941 (2002).
[11] J. Brault, M. Gendry, G. Grenet, G. Hollinger, J. Olivares, B. Salem, T. Benyattou, and G. Bremond, J. Appl. Phys. **92**, 506 (2002).
[12] F. Fossard, F. H. Julien, E. Péronne, A. Alexandrou, J. Brault, and M. Gendry, Infrared Phys. Technol. **42**, 443 (2001).
[13] A. Weber, O. Gauthier-Lafaye, F. H. Julien, J. Brault, M. Gendry, Y. Désieres, and T. Benyattou, Appl. Phys. Lett. **74**, 413 (1999).
[14] S. Fafard and R. Leon, Phys. Rev. B **52**, 5752 (1995).
[15] M. J. Steer, D. J. Mowbray, W. R. Tribe, M. S. Skolnick, M. D. Sturge, M. Hopkinson, A. G. Cullis, C. R. Whitehouse, and R. Murray, Phys. Rev. B **54**, 17 738 (1996).
[16] B. Salem, T. Benyattou, G. Guillot, C. Bru-Chevallier, G. Bremond, C. Monat, G. Hollinger, and M. Gendry, Phys. Rev. B **66**, 193305 (2002).
[17] S. Sauvage, P. Boucaud, F. H. Julien, J.-M. Gérard, and J.-Y. Marzin, J. Appl. Phys. **82**, 3396 (1997).
[18] P. Von-Allmen, M. Berz, G. Petrocelli, F. Reinhart, and G. Harbeke, Semicond. Sci. Technol. **3**, 1211 (1988).
[19] E. Finkman, S. Maimon, V. Immer, G. Bahir, S. E. Schacham, F. Fossard, F. H. Julien, J. Brault, and M. Gendry, Phys. Rev. B **63**, 045323 (2001).
[20] S. E. Schacham, G. Bahir, E. Finkman, F. H. Julien, F. Fossard, J. Brault, and M. Gendry, Infrared Phys. Technol. **44**, 509 (2003).
[21] F. H. Julien and P. Boucaud, in *Optical Intersubband Absorption and Emission in Quantum Structures*, Vol. 344 of NATO Advanced Study Institute, *Optical Spectroscopy of Low-dimensional Semiconductors, Ankara, Turkey, September 1996*, edited by G. Abstreiter (Kluwer Academic, Dordrecht, 1997), pp. 41–61.
[22] C. R. Pidgeon and R. N. Brown, Phys. Rev. **146**, 575 (1966).
[23] K. Boujdaria, S. Ridene, and G. Fishman, Phys. Rev. B **63**, 235302 (2001).
[24] G. Fishman, Phys. Rev. B **52**, 11 132 (1995).
[25] F. Fossard, A. Helman, F. H. Julien, M. Gendry, J. Brault, E. Péronne, A. Alexandrou, S. E. Schacham, and E. Finkman, Physica E (Amsterdam) **17**, 82 (2003).